Observation of a Strong Atom-Dimer Attraction in a Mass-Imbalanced Fermi-Fermi Mixture

Michael Jag,[1,2] Matteo Zaccanti,[1,3] Marko Cetina,[1] Rianne S. Lous,[1,2] Florian Schreck,[1] and Rudolf Grimm[1,2]
[1]Institut für Quantenoptik und Quanteninformation (IQOQI), Österreichische Akademie der Wissenschaften, 6020 Innsbruck, Austria
[2]Institut für Experimentalphysik, Universität Innsbruck, 6020 Innsbruck, Austria
[3]CNR Istituto Nazionale Ottica, 50019 Sesto Fiorentino, Italy
Dmitry S. Petrov,[4] and Jesper Levinsen[5,6]
[4]Université Paris-Sud, CNRS, LPTMS, UMR8626, Orsay F-91405, France
[5]TCM group, Cavendish Laboratory, JJ Thomson Avenue, Cambridge CB3 0HE, United Kingdom
[6]Aarhus Institute of Advanced Studies, Aarhus University, DK-8000 Aarhus C, Denmark
(Received 20 November 2013; published 21 February 2014)

We investigate a mixture of ultracold fermionic ^{40}K atoms and weakly bound ^{6}Li^{40}K dimers on the repulsive side of a heteronuclear atomic Feshbach resonance. By radio-frequency spectroscopy we demonstrate that the normally repulsive atom-dimer interaction is turned into a strong attraction. The phenomenon can be understood as a three-body effect in which two heavy ^{40}K fermions exchange the light ^{6}Li atom, leading to attraction in odd partial-wave channels (mainly p wave). Our observations show that mass imbalance in a fermionic system can profoundly change the character of interactions as compared to the well-established mass-balanced case.

DOI: 10.1103/PhysRevLett.112.075302 PACS numbers: 67.85.Lm, 05.30.Fk, 34.50.Cx, 67.85.Pq

Ultracold fermions with tunable interactions provide remarkable possibilities to model the many-body physics of strongly interacting states of quantum matter under well-controllable conditions [1,2]. Fermionic superfluids, realized by combining two different spin states of a fermionic atomic species and controlling their s-wave interaction through a Feshbach resonance [3], have led to spectacular achievements. Beyond these experimentally well-established fermionic systems, mass imbalance offers an additional degree of freedom, with interesting prospects for new many-body phenomena having no counterpart in the mass-balanced case, such as novel quantum phases or superfluid states in various trapping environments [4–20].

Striking effects of mass imbalance in fermionic systems already emerge at the few-body level. A resonantly interacting three-body system of one light (↓) and two heavy (↑) fermions is known to exhibit bound states depending on the mass ratio $m_\uparrow/m_\downarrow$. While Efimov trimer states require large mass ratios ($m_\uparrow/m_\downarrow > 13.6$), for repulsive interactions, non-Efimovian trimer states can exist in an intermediate regime ($13.6 > m_\uparrow/m_\downarrow > 8.17$) [21]. Below the critical value of 8.17, the last state turns into an atom-dimer scattering resonance in the p-wave channel [21].

The ^{40}K–^{6}Li mixture serves as the prime system for current experiments on tunable mass-imbalanced Fermi-Fermi mixtures [22–24]. The corresponding mass ratio of $m_\uparrow/m_\downarrow \approx 6.64$ lies well in the regime of near-resonant atom-dimer interactions [25,26]: as the most prominent effect, theory predicts a substantial attraction resulting from higher partial waves (mainly p wave) in a regime where one would naively, based on s waves alone, expect a strong repulsion. This also makes the corresponding many-body problem in a ^{40}K–^{6}Li mixture significantly more complicated and much richer than in the widely investigated mass-balanced case.

In this Letter, we investigate the interaction between ^{40}K atoms and weakly bound ^{6}Li–^{40}K dimers near an interspecies Feshbach resonance (FR). We employ radio-frequency (rf) spectroscopy by using two different internal states of ^{40}K, one strongly interacting with the dimers and the other one practically noninteracting [27]. We observe line shifts and collisional broadening and interpret these in terms of the real and imaginary part of the forward-scattering amplitude $f(0)$ for atom-dimer collisions, calculated on the basis of the theoretical approach of Ref. [26]. The comparison between theory and experiment shows excellent agreement and, in particular, demonstrates the predicted atom-dimer attraction on the repulsive side of the interspecies FR.

The interaction of a heavy atom with a heavy-light dimer can be understood in the Born-Oppenheimer approximation, where the atom-dimer potentials are taken to be the eigenenergies of the light atom for a given separation R between the heavy ones. As in the usual double-well problem with tunneling, the state localized near one heavy atom is mixed with the state localized near the other; the symmetric and antisymmetric superpositions lead to the attractive $U_+(R) < 0$ and repulsive $U_-(R) > 0$ potentials, respectively. Note the analogy to the well-known H_2^+

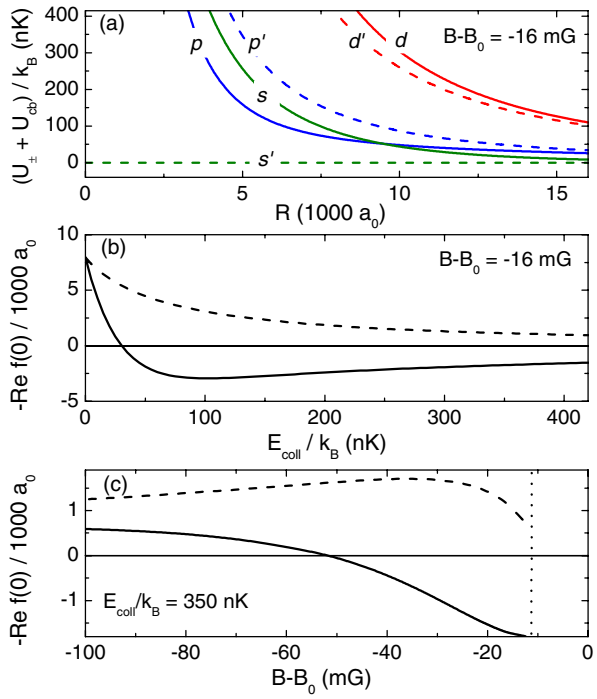

FIG. 1 (color online). Interaction between ^{40}K atoms and ^{6}Li^{40}K dimers near the 155 G interspecies FR. (a) Total interaction potentials as a function of the distance R between the two K atoms for the s, p, and d channels (dashed curves with labels s', p', d' refer to the unmodified centrifugal barriers). Here we have chosen a magnetic detuning of $B - B_0 = -16$ mG, corresponding to an s-wave scattering length of $a = 3500\,a_0$ and to a dimer binding energy of $E_b/k_B = 600$ nK. (b) Real part of the forward-scattering amplitude $f(0)$ as a function of the collision energy E_{coll} (solid line) in comparison with the s-wave contribution (dashed line). (c) Same as in (b), but as a function of the magnetic detuning $B - B_0$ for a fixed collision energy $E_{coll}/k_B = 350$ nK. The dotted line indicates the dimer breakup threshold, $E_{coll} = E_b$.

cation, where the exchange of the electron leads to a symmetric bound state and an antisymmetric unbound state [28]. In our experiment, the heavy particles are identical fermions, making the atom-dimer interaction channel dependent. The symmetric (antisymmetric) state corresponds to odd (even) values of the total angular momentum l [26]. In Fig. 1(a), we plot the total effective potentials $U_\pm + U_{cb}$ (solid lines) and the bare centrifugal barriers $U_{cb} = l(l+1)\hbar^2/m_\uparrow R^2$ (dashed lines) for $l = 0$, 1, and 2 (i.e., s-, p-, and d-wave channels) for typical experimental conditions. At distances on the order of typical de Broglie wavelength, $U_\pm$ can be comparable to U_{cb} and we expect significant interaction effects in nonzero partial waves.

The relevant quantity that characterizes the net effect of all partial waves is the atom-dimer forward scattering amplitude [29–31]

$$f(0) = \sum_{l=0}^{\infty}(2l+1)\left[\frac{\sin 2\delta_l(k_{coll})}{2k_{coll}} + i\frac{\sin^2\delta_l(k_{coll})}{k_{coll}}\right], \quad (1)$$

where $k_{coll} = \sqrt{2\mu_3 E_{coll}}/\hbar$ is the wave number associated with the relative atom-dimer motion and μ_3 is the reduced atom-dimer mass. The phase shifts δ_l for the three lowest partial waves have been computed in Ref. [26], and here, we extend the result to higher ones since they give significant contributions [32]. In Fig. 1(b), we show the resulting $-\mathrm{Re}\,f(0)$ as a function of the collision energy E_{coll} for the same conditions as in Fig. 1(a). In the limit of $E_{coll} \to 0$, the quantity $-\mathrm{Re}\,f(0)$ corresponds to the atom-dimer s-wave scattering length. At $E_{coll} \ll 0.1E_b$, with E_b being the dimer binding energy, s-wave scattering (dashed line) dominates and the net interaction is repulsive, $-\mathrm{Re}\,f(0) > 0$.

For $E_{coll} \gtrsim 0.1E_b$, higher partial-wave contributions lead to a sign reversal of $\mathrm{Re}\,f(0)$, changing the character of the interaction from repulsive into attractive. This sign reversal also appears if, at a fixed collision energy, the magnetic detuning from the FR center is varied, see Fig. 1(c). In the realistic example of Fig. 1(c), the sign reversal takes place at a magnetic detuning of $B - B_0 = -53$ mG, where the binding energy is $E_b/k_B \approx 3.1\ \mu$K, corresponding to roughly ten times the collision energy $E_{coll}/k_B = 350$ nK. The theory lines in Fig. 1(c) stop close to the FR center at the magnetic field detuning where $|E_b| = E_{coll}$ (dotted line), beyond which the inelastic channel of collisional dimer dissociation opens up.

The starting point of our experiments is an optically trapped, near-degenerate Fermi-Fermi mixture of typically 4×10^4 ^{40}K atoms and 1×10^5 ^{6}Li atoms. The preparation procedures are described in our previous work [24,33]. We choose a particular FR that occurs between Li atoms in the lowest Zeeman sublevel Li$|1\rangle$ ($f = 1/2$, $m_f = +1/2$) and K atoms in the third-to-lowest sublevel K$|3\rangle$ ($f = 9/2$, $m_f = -5/2$) [34]. The s-wave interspecies scattering length a can be magnetically tuned as $a = a_{bg}[1 - \Delta/(B - B_0)]$ with $a_{bg} = 63.0\,a_0$ ($a_0 = 1$ Bohr's radius) and $\Delta = 880$ mG [34]. The resonance is rather narrow, as characterized by the length parameter $R^* = 2700\,a_0$ [35]. The position of the FR center near $B \approx 154.7$ G depends on the trap setting, as it includes small shifts induced by the trapping light. For each trap setting, we have calibrated the FR center B_0 with $\lesssim 2$ mG accuracy [32].

We create an atom-dimer mixture by a Feshbach ramp across the resonance and by subsequent purification and spin-manipulation techniques [32]. While the dimers are formed in the Li$|1\rangle$-K$|3\rangle$ spin channel, we initially prepare the free atoms in the second-to-lowest spin state K$|2\rangle$ ($f = 9/2$, $m_f = -7/2$), for which the interaction with the dimers is negligible. The total number of dimers and atoms is 1.5×10^4 and 7×10^3, respectively. The interspecies attraction during the Feshbach ramp results in a collective oscillation of the dimer cloud, which we can take into account by introducing an effective temperature T_{eff} [32]. We use three different trap settings, for which $T_{eff} = 165$ nK, 232 nK, and 370 nK. This corresponds

to mean dimer densities as experienced by the atoms of $\bar{n}_D = 5.2 \times 10^{11}$ cm^{-3}, 8.2×10^{11} cm^{-3}, and 1.4×10^{12} cm^{-3}, respectively.

To investigate the interaction between the K$|3\rangle$ atoms and the Li$|1\rangle$K$|3\rangle$ dimers, we carry out rf spectroscopy. This can be done in two different ways, either by driving the K atoms from the noninteracting state $|2\rangle$ into the interacting state $|3\rangle$ (method A) or vice versa (method B). With our K atoms initially prepared in the state $|2\rangle$, we carry out method A by applying a 1-ms rf pulse. For method B, we rapidly transfer the full K$|2\rangle$ population into K$|3\rangle$ using a short 90– μs preparation pulse without spectral resolution, and then drive the spectrally resolving transition with a 1-ms pulse. Our signal in both cases is the fraction of transferred atoms as a function of the rf detuning $\nu - \nu_0$ with respect to the unperturbed transition frequency ν_0, the latter being determined by the rf spectroscopy in the absence of dimers.

Sample spectra, at a magnetic detuning of $B - B_0 = -20$ mG, are shown in Fig. 2. The spectra recorded by methods A and B (circles and diamonds in Fig. 2) show both a broadening and a peak shift, as compared to the spectra recorded in the absence of dimers (triangles). Although the spectra very close to the FR center reveal asymmetries in their wings, which depend on the method applied, their peak shifts and broadenings are consistent for both methods. In the range of detunings $B - B_0$ studied in the present Letter, the molecular dissociation signal is always well separated from the atomic line (inset of Fig. 2), and thus, does not affect the line shape of the atomic signal.

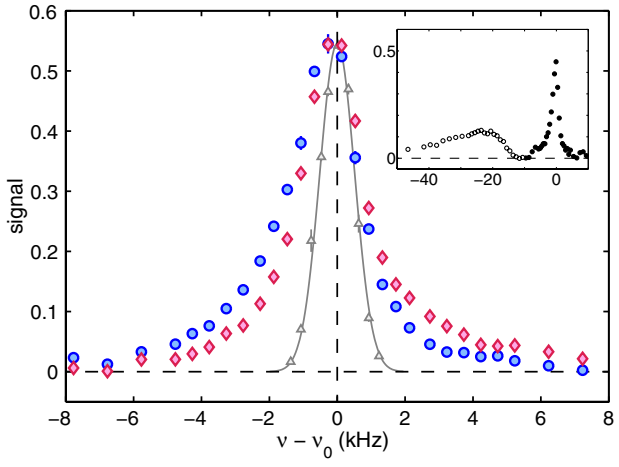

FIG. 2 (color online). Sample rf spectra taken at $B - B_0 = -20$ mG at $T_{\text{eff}} = 232$ nK. The red diamonds (blue circles) show data recorded using method A (B). For reference, the gray triangles show data recorded in the absence of dimers together with a Gaussian fit (gray line). Inset: Spectrum at -17 mG over an extended frequency range. The molecular dissociation signal (open symbols), recorded with 30× increased rf power, is clearly separated from the atomic peak (filled symbols).

Figure 3 shows the widths and peak shifts [36] of the rf spectroscopic signal, recorded by method A, as a function of $B - B_0$ for our three values of T_{eff}. When the FR center is approached, the spectrum broadens and its peak shifts from a positive to a negative rf detuning. With increasing temperature, the corresponding zero crossing shows a trend to move towards larger detunings.

We interpret the obtained results in the framework of the impact theory of pressure-induced effects on spectral lines, which assumes the collisions to be effectively instantaneous. This theory predicts Lorentzian profiles centered near the unperturbed frequency ν_0 whose line shifts and broadenings are proportional to the real and imaginary parts of the thermally averaged atom-dimer forward scattering amplitude $f(0)$ [29–31], respectively. The real part of $f(0)$ shifts the energy of the K atoms, causing an average shift in the frequency of their peak rf response of $\delta\nu = -\hbar\bar{n}_D \text{Re}\langle f(0)\rangle/\mu_3$, where $\langle f(0)\rangle$ denotes the thermal average of $f(0)$ over all atom-dimer collision energies E_{coll}. The red solid lines in Fig. 3 show the theoretical results for $\delta\nu$ for the respective molecule densities and collision energies. The optical theorem relates the imaginary part of $f(0)$ to the average elastic scattering rate τ^{-1} as $\tau^{-1} = 4\pi\hbar\bar{n}_D \text{Im}\langle f(0)\rangle/\mu_3$. The resulting finite lifetime τ of the atoms' wave packets causes Lorentzian broadening with a full width at half maximum (FWHM) $1/(2\pi\tau)$. The blue solid lines in Fig. 3 show the predicted FWHM, including additional broadening due to the finite duration of our rf pulse [37].

The collisional broadening yields information on the elastic scattering rate. At typical detunings of

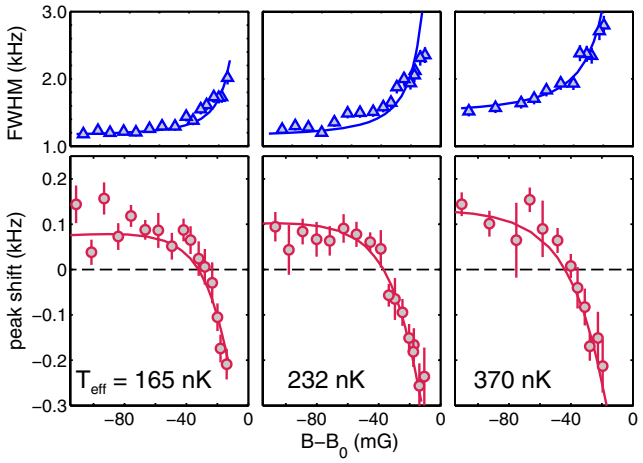

FIG. 3 (color online). Widths (blue triangles) and peak shifts (red circles) extracted from the rf spectra as a function of the magnetic field detuning $B - B_0$ for the three different values of T_{eff}. The lines are the corresponding theoretical predictions. To account for fluctuations in the dimer number of different spectra, the widths and peak shifts are scaled to a dimer number of 15 000, which is typical for all spectra.

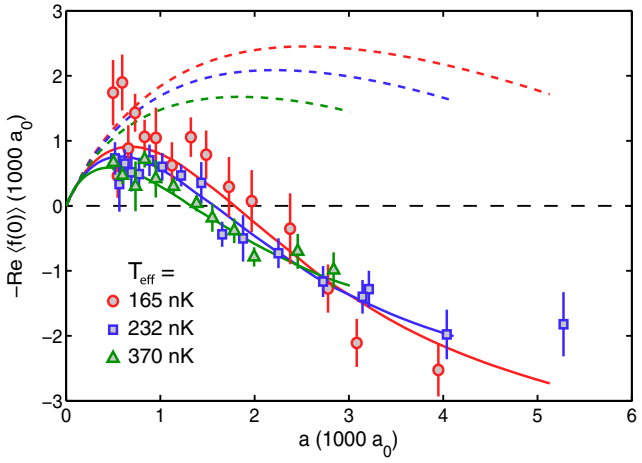

FIG. 4 (color online). Real part of the atom-dimer forward-scattering amplitude as a function of the atom-atom scattering length a for the three different values of T_{eff}. The symbols and the lines show the data and the theoretical predictions from Fig. 3. For comparison, the dashed lines indicate the respective s-wave contributions. The theoretical lines stop at $k_{\mathrm{B}}T_{\mathrm{eff}} = E_{\mathrm{b}}/2$.

$B - B_0 \approx -20$ mG, our data show an elastic atom-dimer scattering rate on the order of $1/(100\ \mu\mathrm{s})$. A comparison with the observed dimer decay rate of about $1/(5\ \mathrm{ms})$ gives a lower limit for the ratio of elastic to inelastic atom-dimer collisions of 50. We note that, in our system, the dimers spontaneously dissociate on a time scale of about 10 ms [34].

The comparison between the experimentally observed and the theoretically calculated line shifts and broadenings shows remarkable agreement over the whole parameter range investigated. The somewhat asymmetric spectral wings are beyond the impact theory [38] and, thus, cannot be reproduced. Indeed, a substantial contribution to the wings comes from the photon emission and absorption events for which K atoms find themselves inside the atom-dimer interaction range, i.e., during atom-dimer collisions, which are assumed instantaneous in the impact theory. It is, then, understood that, for example, the left "attractive" wing of the B spectrum is larger than that of the A spectrum. Since, in the former case, potassium atoms are initially attracted by dimers, the probability to find them near dimers is enhanced. Effects that are beyond the impact theory become more pronounced as we approach the FR because of the increased atom-dimer collision time.

Finally, we discuss the interaction strength in our mixture in terms of $-\mathrm{Re}\,\langle f(0)\rangle$, which characterizes the interactions in a way that is analogous to a in the s-wave mean-field picture. We use the experimental peak-shift data from Fig. 3 to extract $-\mathrm{Re}\,\langle f(0)\rangle$ and plot it together with the corresponding theoretical results in Fig. 4. The sign reversal shows up for values of a being somewhat below $2000\,a_0$, with the expected temperature dependence of the zero crossing. For $a \approx 4000\,a_0$, the attractive interaction already corresponds to about $-2000\,a_0$. For even larger values of a, we would enter the more complicated regime of collisional dimer dissociation, which is beyond the scope of the present investigations. We note, however, that rf spectra acquired more deeply in the strongly interacting regime show strongly asymmetric line shapes and have peaks shifted to even larger negative detunings.

In conclusion, we have demonstrated a three-body phenomenon in a mixture of heavy and light fermions, which leads to a sign reversal of the atom-dimer interaction near a FR, turning repulsion into a strong attraction. The effect is due to higher partial-wave (mainly p wave) contributions, which are present even at very low collision energies in the nanokelvin regime. Remarkably, this few-body effect changes the character of the interaction without introducing detrimental losses. In contrast to few-body phenomena of the Efimov type [39], the centrifugal barrier still protects the atoms from approaching each other too closely. The resulting collisional stability is a promising feature for many-body physics in Fermi-Fermi mixtures.

Our work lays the ground for a wealth of future studies on mass-imbalanced fermionic mixtures in the strongly interacting regime. Asymmetric phases with coexisting dimers and heavy atoms are energetically favored in a way not present in mass-balanced systems [12]. Related mechanisms in quantum-degenerate situations may lead to exotic new many-body effects, including the emergence of imbalanced superfluids [12], the condensation into nonzero momentum states [11], and the appearance of p-wave superfluidity of heavy atoms mediated by light atoms [40]. On the few-body side, a direct prospect for our K-Li system is to confine the K atoms in an optical lattice, which is predicted to lead to the formation of stable trimer states [14,20,25].

We acknowledge funding by the Austrian Science Fund FWF the SFB FoQuS (F40-P04). M. Z. was supported by the FWF within the Lise Meitner Program (No. M1318), D. S. P. by the Institut Francilien de Recherche sur les Atomes Froids (IFRAF), and J. L. acknowledges support from the Carlsberg Foundation.

[1] S. Giorgini, L. P. Pitaevskii, and S. Stringari, Rev. Mod. Phys. **80**, 1215 (2008).
[2] I. Bloch, J. Dalibard, and W. Zwerger, Rev. Mod. Phys. **80**, 885 (2008).
[3] C. Chin, R. Grimm, P. S. Julienne, and E. Tiesinga, Rev. Mod. Phys. **82**, 1225 (2010).
[4] M. Iskin and C. A. R. Sá de Melo, Phys. Rev. Lett. **97**, 100404 (2006).
[5] I. Bausmerth, A. Recati, and S. Stringari, Phys. Rev. A **79**, 043622 (2009).
[6] A. Gezerlis, S. Gandolfi, K. E. Schmidt, and J. Carlson, Phys. Rev. Lett. **103**, 060403 (2009).

[7] C. W. von Keyserlingk and G. J. Conduit, Phys. Rev. A **83**, 053625 (2011).
[8] A. Sotnikov, D. Cocks, and W. Hofstetter, Phys. Rev. Lett. **109**, 065301 (2012).
[9] X. Cui and T.-L. Ho, Phys. Rev. Lett. **110**, 165302 (2013).
[10] K. B. Gubbels, J. E. Baarsma, and H. T. C. Stoof, Phys. Rev. Lett. **103**, 195301 (2009).
[11] C. J. M. Mathy, M. M. Parish, and D. A. Huse, Phys. Rev. Lett. **106**, 166404 (2011).
[12] R. Qi and H. Zhai, Phys. Rev. A **85**, 041603(R) (2012).
[13] K. M. Daily and D. Blume, Phys. Rev. A **85**, 013609 (2012).
[14] D. S. Petrov, G. E. Astrakharchik, D. J. Papoular, C. Salomon, and G. V. Shlyapnikov, Phys. Rev. Lett. **99**, 130407 (2007).
[15] M. A. Baranov, C. Lobo, and G. V. Shlyapnikov, Phys. Rev. A **78**, 033620 (2008).
[16] C. Sanchez-Castro and K. S. Bedell, Phys. Rev. B **43**, 12874 (1991).
[17] G. Orso, E. Burovski, and T. Jolicoeur, Phys. Rev. Lett. **104**, 065301 (2010).
[18] M. Dalmonte, K. Dieckmann, T. Roscilde, C. Hartl, A. E. Feiguin, U. Schollwöck, and F. Heidrich-Meisner, Phys. Rev. A **85**, 063608 (2012).
[19] Y. Nishida and S. Tan, Phys. Rev. Lett. **101**, 170401 (2008).
[20] Y. Nishida and S. Tan, Phys. Rev. A **79**, 060701(R) (2009).
[21] O. I. Kartavtsev and A. V. Malykh, J. Phys. B **40**, 1429 (2007).
[22] E. Wille, F. M. Spiegelhalder, G. Kerner, D. Naik, A. Trenkwalder, G. Hendl, F. Schreck, R. Grimm, T. G. Tiecke, J. T. M. Walraven, *et al.*, Phys. Rev. Lett. **100**, 053201 (2008).
[23] L. Costa, J. Brachmann, A.-C. Voigt, C. Hahn, M. Taglieber, T. W. Hänsch, and K. Dieckmann, Phys. Rev. Lett. **105**, 123201 (2010).
[24] A. Trenkwalder, C. Kohstall, M. Zaccanti, D. Naik, A. I. Sidorov, F. Schreck, and R. Grimm, Phys. Rev. Lett. **106**, 115304 (2011).
[25] J. Levinsen, T. G. Tiecke, J. T. M. Walraven, and D. S. Petrov, Phys. Rev. Lett. **103**, 153202 (2009).
[26] J. Levinsen and D. Petrov, Eur. Phys. J. D **65**, 67 (2011).
[27] C. Kohstall, M. Zaccanti, M. Jag, A. Trenkwalder, P. Massignan, G. M. Bruun, F. Schreck, and R. Grimm, Nature (London) **485**, 615 (2012).
[28] L. Pauling, Chem. Rev. **5**, 173 (1928).
[29] I. I. Sobelman, *An Introduction to the Theory of Atomic Spectra* (Pergamon Press, Oxford, 1972).
[30] M. Baranger, Phys. Rev. **111**, 481 (1958).
[31] M. Baranger, Phys. Rev. **112**, 855 (1958).
[32] See Supplemental Material at http://link.aps.org/supplemental/10.1103/PhysRevLett.112.075302 for details on the calibration of the FR center, the preparation of the atom-dimer mixture, the determination of the temperatures and the densities, and the effect of higher partial waves on the forward-scattering amplitude.
[33] F. M. Spiegelhalder, A. Trenkwalder, D. Naik, G. Kerner, E. Wille, G. Hendl, F. Schreck, and R. Grimm, Phys. Rev. A **81**, 043637 (2010).
[34] D. Naik, A. Trenkwalder, C. Kohstall, F. M. Spiegelhalder, M. Zaccanti, G. Hendl, F. Schreck, R. Grimm, T. Hanna, and P. Julienne, Eur. Phys. J. D **65**, 55 (2011).
[35] D. S. Petrov, Phys. Rev. Lett. **93**, 143201 (2004).
[36] To determine the peak shift and the width, we apply a double-Gaussian fit to the spectra. From the fit, we identify the rf detuning of maximum signal and the width.
[37] The finite duration of our rf pulse causes an additional Gaussian broadening of typically 1.2 kHz (FWHM).
[38] J. Szudy and W. E. Baylis, Phys. Rep. **266**, 127 (1996).
[39] F. Ferlaino, A. Zenesini, M. Berninger, B. Huang, H.-C. Nägerl, and R. Grimm, Few-Body Syst. **51**, 113 (2011).
[40] Y. Nishida, Phys. Rev. A **79**, 013629 (2009).